articles

molecular pharmaceutics

Prostate-Specific Membrane Antigen Targeted Imaging and Therapy of Prostate Cancer Using a PSMA Inhibitor as a Homing Ligand

Sumith A. Kularatne,[†] Kevin Wang,[‡] Hari-Krishna R. Santhapuram,[‡] and Philip S. Low*[,†]

Department of Chemistry, Purdue University, 560 Oval Drive, West Lafayette, Indiana 47907, and Endocyte, Inc., 3000 Kent Avenue, West Lafayette, Indiana 47906

Received February 25, 2009; Revised Manuscript Received April 9, 2009; Accepted April 11, 2009

Abstract: Prostate cancer (PCa) is a major cause of mortality and morbidity in Western society today. Current methods for detecting PCa are limited, leaving most early malignancies undiagnosed and sites of metastasis in advanced disease undetected. Major deficiencies also exist in the treatment of PCa, especially metastatic disease. In an effort to improve both detection and therapy of PCa, we have developed a PSMA-targeted ligand that delivers attached imaging and therapeutic agents selectively to PCa cells without targeting normal cells. The PSMA-targeted radioimaging agent (DUPA−^{99m}Tc) was found to bind PSMA-positive human PCa cells (LNCaP cell line) with nanomolar affinity (K_D = 14 nM). Imaging and biodistribution studies revealed that DUPA−^{99m}Tc localizes primarily to LNCaP cell tumor xenografts in nu/nu mice (% injected dose/gram = 11.3 at 4 h postinjection; tumor-to-muscle ratio = 75:1). Two PSMA-targeted optical imaging agents (DUPA−FITC and DUPA−rhodamine B) were also shown to efficiently label PCa cells and to internalize and traffic to intracellular endosomes. A PSMA-targeted chemotherapeutic agent (DUPA−TubH) was demonstrated to kill PSMA-positive LNCaP cells in culture (IC_{50} = 3 nM) and to eliminate established tumor xenografts in nu/nu mice with no detectable weight loss. Blockade of tumor targeting upon administration of excess PSMA inhibitor (PMPA) and the absence of targeting to PSMA-negative tumors confirmed the specificity of each of the above targeted reagents for PSMA. Tandem use of the imaging and therapeutic agents targeted to the same receptor could allow detection, staging, monitoring, and treatment of PCa with improved accuracy and efficacy.

Keywords: Prostate-specific membrane antigen; PSMA-targeted imaging and therapy; radioimaging and optical imaging of prostate cancer; tubulysin prodrug; diagnosis of prostate cancer; chemotherapy for prostate cancer

Introduction

Prostate cancer (PCa) is the most common male malignancy in western society, amounting to ~230,000 new cases/year in the US.[1] More males die from PCa (>30,000/year) than any other malignancy except lung cancer,[1] and the cumulative cost of treating PCa patients has been estimated at $8−10 billion/year in the US.[2] Advanced stages of PCa can also significantly impact quality of life due to bone disintegration, pain, obstruction of urination, and erectile dysfunction among other disorders.[3]

Although neoplastic transformation begins in the prostate gland, malignant cells can eventually metastasize to other parts of the body, including bones, rectum, and bladder. Because metastatic PCa is difficult to treat, early detection

* Corresponding author. Mailing address: Department of Chemistry, Purdue University, 560 Oval Drive, West Lafayette, IN 47907. Phone: 765-494-5273. Fax: 765-494-5272. E-mail: plow@purdue.edu.

[†] Purdue University.

[‡] Endocyte, Inc.

(1) Jemal, A.; Siegel, R.; Ward, E. Cancer statistics 2008. *Ca—Cancer J. Clin.* **2008**, *58*, 71–96.

10.1021/mp900069d CCC: $40.75
Published on Web 04/12/2009

constitutes the most effective strategy for minimizing disease-related morbidity and mortality. Early diagnosis of PCa is most commonly achieved by digital rectal exam, blood test for prostate specific antigen (PSA), or a prostate biopsy.[4] However, only more advanced stages of disease can be detected by a digital rectal exam[5] and prostate biopsies can be expensive and painful.[6] Further, the accuracy of the PSA test has been criticized[7] due to its elevation during benign prostatic hypertrophy (BPH) or prostatitis and due to its decline during treatment for BPH or baldness.[8] Although transrectal ultrasound together with magnetic resonance imaging (MRI) and computerized tomography (CT) can effectively reveal the extent of prostate enlargement and growth asymmetry, these exams are too expensive for routine screening and may not distinguish malignant disease from BPH.[9] Clearly, better methods for assessing onset and spread of PCa could greatly reduce the frequency of advanced stage disease.

Treatment for PCa most commonly involves surgery, radiation therapy, hormone administration, and/or chemotherapy. Unfortunately, none of these therapies is highly effective against metastatic disease, and each has sufficient disadvantages that patients often decline their use. While localized PCa can be treated by removal of malignant tissue,[10] radical prostatectomy may result in loss of urinary control and impotence.[11] Radiation therapy can also cause impotence, rectal bleeding,[3] and increased risk of colon and bladder cancer,[12] and treatment of invasive or metastatic PCa is often limited to palliative hormonal therapy and/or chemotherapy. While hormonal treatment induces remission of hormonally responsive cancer, the longevity of tumor remission is limited and it is not without significant toxicity, including liver damage, cardiovascular disease, weight gain, and osteoporosis.[13] And although chemotherapy (e.g., mitoxantrone) may also extend lifespan,[14] side effects of such antimitotic drugs often outweigh their benefits. Therefore, safer and more potent methods of treating PCa are widely needed.

In an effort to improve both detection and treatment of PCa, we initiated a search for low molecular weight ligands that would selectively target attached drugs to PCa cells without promoting their uptake by healthy cells. Prostate-specific membrane antigen (PSMA, folate hydrolase I, glutamate carboxypeptidase II), a plasma membrane-associated protein,[15] is overexpressed on the vast majority of PCa.[16] While the physiological function of PSMA remains controversial, its expression is largely limited to PCa cells,[16,17] where malignant transformation leads not only to its up-regulation but also to its translocation from internal organelles to the cell surface. For unknown reasons, PSMA is also expressed in the neovasculature of most other solid tumors (but not in the vasculature of healthy tissues),[16,18] and in the kidneys, albeit at significantly lower levels in human kidneys[16,17] than murine kidneys.[19] For drug targeting applications, perhaps the most important characteristic of PSMA is that it undergoes internalization through clathrin-coated pits and rapidly recycles to the cell surface for

(2) Wilson, L. S.; Tesoro, R.; Elkin, E. P. Cumulative cost pattern comparison of prostate cancer treatments. *Cancer* **2007**, *109*, 518–527.
(3) Katz, A. Quality of life for men with prostate cancer. *Cancer Nurs.* **2007**, *30*, 302–308.
(4) Zeller, J. L. Grading of prostate cancer. *JAMA, J. Am. Med. Assoc.* **2007**, *298*, 1596.
(5) Chodak, M. D.; Keller, P.; Schoenberg, H. W. Assessment of screening for prostate cancer using the digital rectal examination. *J. Urol.* **1989**, *141*, 1136–1138.
(6) Essink-Bot, M.; de Koning, H. J.; Nijs, H. G. J.; Kirkels, W. J.; van der Mass, P. J.; Schroder, F. H. Short term effects of population-based screening for prostate cancer on health-related quality of life. *J. Natl. Cancer Inst.* **1998**, *90*, 925–931.
(7) Linn, M. M.; Ball, R. A.; Maradiegue, A. Prostate-specific antigen screening: Friend or foe? *Urol. Nurs.* **2007**, *27*, 481–489.
(8) D'Amico, A. V.; Roehrborn, C. G. Effect of 1 mg/day finasteride on concentration of serum prostate specific antigen in men with androgenic alopecia: a randomized controlled trial. *Lancet Oncol.* **2007**, *8*, 21–25.
(9) Holves, A. M.; Heesakkers, R. A. M.; Adang, E. M. The diagnostic accuracy of CT and MRI in the pelvis of lymph nodes in patients with prostate cancer: a meta-analysis. *Clin. Radiol.* **2008**, *63*, 387–95.
(10) Bill-Axelson, A.; Andersson, S.-O.; Bratell, S. Radical prostatectomy versus watchful waiting in early prostate cancer. *N. Engl. J. Med.* **2005**, *352*, 1977–1984.
(11) Weber, B. A.; Robert, B. L.; Chumbler, N. R.; Mills, T. L.; Algood, C. B. Urinary, sexual and bowel dysfunction and bother after radical prostatectomy. *Urol. Nurs.* **2007**, *27*, 527–533.
(12) Brenner, D. J.; Curtis, R. E.; Ron, E. Second malignancies in prostate carcinoma patients after radiotherapy compared with surgery. *Cancer* **2000**, *88*, 398–406.
(13) Kumar, R. J.; Bargawi, A. Crawford ED. Adverse events associated with hormonal therapy for prostate cancer. *Rev. Urol.* **2005**, *7*, 37–43.
(14) Hsiao, C.; Li, T.-K.; Chan, Y.-L. WRC-213, an L-methionine-conjugated mitoxantrone derivative, displays anticancer activity with reduced cardiotoxicity and drug resistance: identification of topoisomerase II inhibition and apoptotic machinery. *Biochem. Pharmacol.* **2008**, *75*, 847–856.
(15) Gang, M. C.; Chang, S. S.; Sadelain, M.; Bander, N. H.; Heston, W. D. Prostate specific membrane antigen (PSMA)-specific monoclonal antibodies in the treatment of prostate and other cancers. *Cancer Metastasis Rev.* **1999**, *18*, 483–490.
(16) Ghosh, A.; Heston, W. D. Tumor target prostate specific membrane antigen (PSMA) and its regulation in prostate cancer. *J. Cell Biochem.* **2004**, *91*, 528–539.
(17) Silver, D. A.; Pellicer, I.; Fair, W. R.; Heston, W. D.; Cordon-Cardo, C. Prostate-specific membrane antigen expression in normal and malignant human tissues. *Clin. Cancer Res.* **1997**, *3*, 81–85.
(18) Chang, S. S.; O'Keefe, D. S.; Bacich, D. J.; Reuter, V. E.; Heston, W. D.; Gaudin, P. B. Prostate-specific membrane antigen is produced in tumor-associated neovasculature. *Clin. Cancer Res.* **1999**, *5*, 2674–2681.
(19) Slusher, B. S.; Tsai, G.; Yoo, G.; Coyle, J. T. Immunocytochemical localization of the N-acetyl-aspartyl-glutamate (NAAG) hydrolyzing enzyme N-acetylated α-linked acidic dipeptidase (NAALADase). *J. Comp. Neurol.* **1992**, *315*, 217–229.

additional rounds of internalization.[20] Collectively, these unique features render PSMA an excellent candidate for use in tumor-targeted drug delivery.

For the above reasons, a variety of efforts have been made to develop PSMA-targeted imaging agents for use in the diagnosis and monitoring of PCa.[21−27] Indeed, a variety of low molecular weight inhibitors of PSMA have been radiolabeled and used to image human PCa xenografts (LNCaP and PC-3 cell lines) in athymic nude mice.[23,28−30] In this report, we describe the design and use of a PSMA-specific ligand for the selective delivery of both imaging and therapeutic agents to a human PCa xenograft (LNCaP cells) in nu/nu mice. We also demonstrate that the PSMA-specific ligand can deliver sufficient tubulysin, a microtubule inhibitor, to established solid LNCaP tumors in athymic mice to induce their long-term remission without causing measurable toxicity to healthy tissues.

Experimental Section

Materials. Sodium pertechnetate was purchased from Cardinal Health (Indianapolis, IN). [^{3}H]-Thymidine was obtained from Moravek Biochemicals (Brea, CA), and 2-(phosphonomethyl)-pentanedioic acid (PMPA) was from Axxora Platform (San Diego, CA). Tubulysin B was provided by Endocyte Inc. (W. Lafayette, IN). HC Matrigel was obtained from BD Bioscience (San Jose, CA). All other chemicals were purchased from major suppliers.

Synthesis of DUPA Conjugates. DUPA−^{99m}Tc was synthesized as described in the companion paper (DOI 10.1021/mp9000712) to this report.[31] The synthesis of DUPA−TubH will be described in detail elsewhere (manuscript in preparation). DUPA−FITC was synthesized by solid phase methodology as follows (see Scheme 1). Universal NovaTag resin (50 mg, 0.53 mM) was swollenwith dichloromethane (DCM) (3 mL) followed by dimethylformamide (DMF, 3 mL). A solution of 20% piperidine in DMF (3 × 3 mL) was added to the resin, and argon was bubbled for 5 min. The resin was washed with DMF (3 × 3 mL) and isopropyl alcohol (*i*-PrOH, 3 × 3 mL). After swelling the resin in DMF, a solution of DUPA(O^{t}Bu)-OH (1.5 equiv), HATU (2.5 equiv) and DIPEA (4.0 equiv) in DMF was added. Argon was bubbled for 2 h, and resin was washed with DMF (3 × 3 mL) and *i*-PrOH (3 × 3 mL). After swelling the resin in DCM, a solution of 1 M HOBt in DCM/trifluoroethane (TFE) (1:1) (2 × 3 mL) was added. Argon was bubbled for 1 h, the solvent was removed and resin was washed with DMF (3 × 3 mL) and *i*-PrOH (3 × 3 mL). After swelling the resin in DMF, a solution of Fmoc-Phe-OH (2.5 equiv), HATU (2.5 equiv) and DIPEA (4.0 equiv) in DMF was added. Argon was bubbled for 2 h, and resin was washed with DMF (3 × 3 mL) and *i*-PrOH (3 × 3 mL). The above sequence was repeated for 2 more coupling steps for addition of 8-aminooctanoic acid and fluorescein isothiocyanate or rhodamine B isothiocyanate. Final compound was cleaved from the resin using a trifluoroacetic acid (TFA): H_2O:triisopropylsilane:cocktail (95:2.5:2.5) and concentrated under vacuum. The concentrated product was precipitated in diethyl ether and dried under vacuum. The crude product was purified using preparative RP-HPLC [λ = 488 nm; solvent gradient: 1% B to 80% B in 25 min, 80% B wash 30 min run; A = 10 mM NH_4OAc, pH = 7; B = acetonitrile (ACN)]. ACN was removed under vacuum, and pure fractions were freeze-dried to yield DUPA−FITC as a brownish-orange solid. RP-HPLC: t_R = 8.0 min (A = 10 mM NH_4OAc, pH = 7.0; B = ACN, solvent gradient: 1%

(20) Liu, H.; Rajasekaran, A. K.; Moy, P. Constitutive and antibody-induced internalization of prostate-specific membrane antigen. *Cancer Res.* **1998**, *58*, 4055–4060.
(21) Sodee, D. B.; Ellis, R. J.; Samuels, M. A. Prostate cancer and prostate bed SPECT imaging with ProstaScint: Semiquantitative correlation with prostatic biopsy results. *Prostate* **1998**, *37*, 140–148.
(22) Milowsky, M. I.; Nanus, D. M.; Kostakoglu, L. Vascular targeted therapy with anti-prostate-specific membrane antigen monoclonal antibody J591 in advanced solid tumors. *J. Clin. Oncol.* **2007**, *25*, 540–547.
(23) Zhou, J.; Neale, J. H.; Pomper, M. G.; Kozikowski, A. P. NAAG peptidase inhibitors and their potential for diagnosis and therapy. *Nat. Rev.* **2005**, *4*, 1015–1026.
(24) Misra, P.; Valerie, H.; Pannier, N.; Maison, W.; Frangioni, J. V. Production of multimeric prostate-specific membrane antigen small-molecule radiotracers using a solid-phase 99mTc preloading strategy. *J. Nucl. Med.* **2007**, *48*, 1379–1389.
(25) Tang, H.; Brown, M.; Ye, Y. Prostate targeting ligands based on N-acetylated á-linked acidic dipeptidase. *Biochem. Biophys. Res. Commun.* **2003**, *307*, 8–14.
(26) Humblet, V.; Lapidus, R.; Williams, L. High-affinity near-infrared fluorescent small-molecule contrast agents for in vivo imaging of prostate-specific membrane antigen. *Mol. Imaging* **2005**, *4*, 448–462.
(27) Liu, T.; Wu, L.; Kazak, M.; Berkman, C. E. Cell-surface labeling and internalization by a fluorescent inhibitor of prostate-specific membrane antigen. *Prostate* **2008**, *68*, 955–964.
(28) Mease, R. C.; Dusich, C. L.; Foss, C. A. N-[N-[(S)-1,3-dicarboxypropyl]carbamoyl]-4-[^{18}F]fluorobenzyl-Lcysteine, [^{18}F]DCFBC: a new imaging probe for prostate cancer. *Clin. Cancer Res.* **2008**, *14*, 3036–3043.
(29) Banerjee, S. R.; Foss, A. C.; Castanares, M. Synthesis and evaluation of technetium-99m- and rhenium-labeled inhibitors of the prostate-specific membrane antigen (PSMA). *J. Med. Chem.* **2008**, *51*, 4504–4517.
(30) Chen, Y.; Foss, C. A.; Byun, Y. Radiohalogenated prostate-specific membrane antigen (PSMA)-based ureas as imaging agents for prostate cancer. *J. Med. Chem.* **2008**, *51*, 7933–7943.
(31) Kularatne, S. A.; Zhou, Z.; Yang, J.; Post, C. B.; Low, P. S. Design, synthesis, and preclinical evaluation of prostate-specific membrane antigen targeted ^{99m}Tc-radioimaging agents *Mol. Pharmaceutics*. DOI 10.1021/mp9000712.
(32) Leamon, C. P.; Parker, M. A.; Vlahoc, I. R. Synthesis and biological evaluation of EC20: a new folate-derived 99mTc-based radiopharmaceutical. *Bioconjugate Chem.* **2002**, *13*, 1200–1210.
(33) Leamon, C. P.; Reddy, J. A.; Wetzel, M. Folate targeting enables durable and specific antitumor responses from a therapeutically null tubulysin B analogue. *Cancer Res.* **2008**, *68*, 9839–9844.
(34) He, W.; Kularatne, S. A.; Kelli, K. R. Quantitation of circulating tumor cells in blood samples from ovarian and prostate cancer patients using tumor-specific fluorescent ligands. *Int. J. Cancer* **2008**, *123*, 1968–1973.

Scheme 1[a]

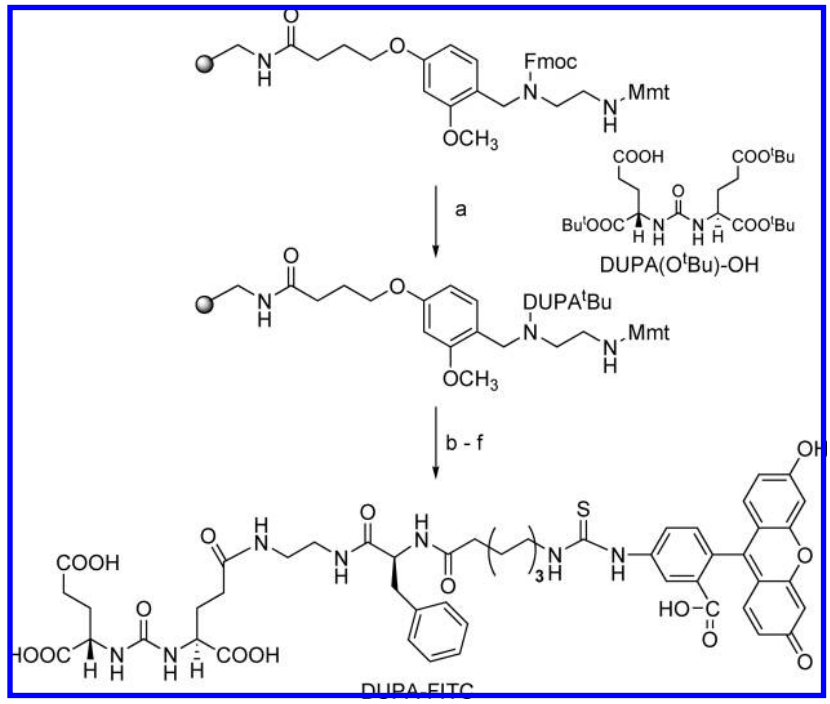

[a] Reagents and conditions: (a) (i) 20% piperidine/DMF, rt, 10 min; (ii) DUPA(O^{t}Bu)-OH, HATU, DIPEA, 2 h; (b) 1 M HOBt in DCM/TFE (1:1), 1 h; (c) (i) 20% piperidine/DMF, rt, 10 min; (ii) Fmoc-Phe-OH, HATU, DIPEA, 2 h; (d) (i) 20% piperidine/DMF, rt, 10 min; (ii) Fmoc-8-aminooctanoic (EAO) acid, HATU, DIPEA, 2 h; (e) (i) 20% piperidine/DMF, rt, 10 min; (ii) fluorescein isothiocyanate (FITC) or rhodamine B isothiocyanate, DIPEA/DMF; (f) TFA/H_2O/TIPS (95:2.5:2.5), 30 min.

B to 50% B in 10 min, 80% B wash 15 min run). ^{1}H NMR (DMSO-d_6/D_2O): δ 0.98−1.27 (ms, 9H); 1.45 (b, 3H); 1.68−1.85 (ms, 11H); 2.03 (m, 8H); 2.6−3.44 (ms, 12H); 3.82 (b, 2H); 4.35 (m, 1H); 6.53 (d, J = 8.1 Hz, 2H), 6.61 (dd, J = 5.3, 3.5 Hz, 2H); 6.64 (s, 2H); 7.05 (d, J = 8.2 Hz, 2H), 7.19 (m, 5H); 7.76 (d, J = 8.0 Hz, 1H); 8.38 (s, 1H). HRMS (ESI) (m/z): $(M + H)^+$ calcd for $C_{51}H_{59}N_7O_{15}S$, 1040.3712, found, 1040.3702. UV/vis: λ_{max} = 491 nm.

Characterization of DUPA−Rhodamine B. Purple solid, analytical HPLC: t_R = 8.4 min (A = 10 mM NH_4OAc, pH = 7.0; B = CAN, solvent gradient: 1% B to 70% B in 10 min, 80% B wash 15 min run); 1.08−1.53 (21H); 1.65 (b, 4H); 1.84−2.20 (ms, 6H); 2.83 (m, 1H); 2.97 (b, 3H); 3.01 (b, 3H); 3.36 (b, 9H); 3.90 (b, 2H); 4.62 (s, 1H); 6.52 (m, 5H); 7.18 (m, 5H); 7.82 (m, 2H); 8.20 (m, 1H); 8.35 (s, 1H). LRMS (ESI) (m/z): $(M)^+$ calcd for $C_{59}H_{76}N_9O_{13}S$, 1151.35, found, 1151.19. UV/vis: λ_{max} = 555 nm.

Cell Culture and Animals. LNCaP, KB, and A549 cells were obtained from American Type Culture Collection. Cells were grown as a monolayer using 1640 RPMI medium containing 10% heat-inactivated fetal bovine serum, sodium pyruvate (100 mM) and 1% penicillin streptomycin in a 5% CO_2:95% air-humidified atmosphere at 37 °C.

Male *nu/nu* mice were purchased from NCI Charles River Laboratories and maintained on normal rodent diet during the study.

Preparation of DUPA−^{99m}Tc Radioimaging Agent. A solution of sodium pertechnetate (1.0 mL, 15 mCi) was added to a vial containing a lyophilized mixture of DUPA−chelate conjugate (0.14 mg), sodium α-D-glucoheptonate dihydrate (80 mg), stannous chloride dihydrate (0.80 mg), and sufficient NaOH to achieve a pH of 7.2 upon rehydration with water. The vial was heated in a boiling water bath for 18 min and then cooled to rt before use.

Binding Affinity and Specificity of DUPA−^{99m}Tc. LNCaP cells (150,000 cells/well in 500 μL) were seeded into 24-well Falcon plates and allowed cells to form monolayers over 48 h. Spent medium in each well was replaced with fresh medium (0.5 mL) containing increasing concentrations of DUPA−^{99m}Tc in the presence or absence of 100-fold excess (ex) PMPA. After incubating for 1 h at 37 °C, cells were rinsed with medium (2× 1.0 mL) and tris buffer (1× 1.0 mL). After dissolving cells in 0.25 M $NaOH_{(aq)}$ (0.5 mL), cells were transferred into individual γ-counter tubes and radioactivity was counted using a γ-counter (Packard, Packard Instrument Company). K_D was calculated by plotting bound radioactivity versus the concentration of radiotracer using GraphPad Prism 4.

Flow Cytometry. LNCaP cells were seeded into a T75 flask and allowed to form a monolayer over 48 h. After trypsin digestion, release cells were transferred into centrifuge tubes (1×10^6 cells/tube) and centrifuged. The medium was replaced with fresh medium containing DUPA−FITC (100 nM) in the presence or absence of 100-fold excess PMPA and incubated for 1 h at 37 °C. After rinsing with fresh medium (2× 1.0 mL) and tris buffer (1× 1.0 mL), cells were resuspended in PBS (1.0 mL) and cell bound fluorescence was analyzed (500,000 cells/sample) using a flow cytometer

(Cytomics F500, Beckman Coulter). Untreated LNCaP cells in PBS served as a negative control.

Confocal Microscopy. LNCaP cells (100,000 cells/well in 1 mL) were seeded into poly-D-lysine microwell Petri dishes and allowed cells to form monolayers over 24 h. Spent medium was replaced with fresh medium containing DUPA−FITC (100 nM) or DUPA−rhodamine (100 nM) in the presence or absence of 100-fold excess PMPA and cells were incubated for 1 h at 37 °C. After rinsing with fresh medium (2× 1.0 mL) and PBS (1× 1.0 mL), confocal images were acquired using a confocal microscopy (FV 1000, Olympus).

Tumor Models, Imaging, and Biodistribution Studies. Five-week-old male nu/nu mice were inoculated subcutaneously with LNCaP cells (5.0×10^6/mouse in 50% HC Matrigel), KB cells, or A549 (1.0×10^6/mouse in RPMI medium) on their shoulders. Growth of the tumors was measured in two perpendicular directions every 2 days using a caliper (body weights were monitored on the same schedule), and the volumes of the tumors were calculated as $0.5 \times L \times W^2$ (L = longest axis and W = axis perpendicular to L in millimeters). Once tumors reached between 400 and 500 mm^3 in volume, animals were treated with DUPA−^{99m}Tc (67 nmol, 150 μCi) in saline (100 μL). After 4 h, animals were sacrificed by CO_2 asphyxiation. Images were acquired by a Kodak Imaging Station (In-Vivo FX, Eastman Kodak Company) in combination with CCD camera and Kodak molecular imaging software (version 4.0). Radioimages: illumination source = radio isotope, acquisition time = 3 min, *f*-stop = 4, focal plane = 5, FOV = 160, binning = 4. White light images: illumination source = white light transillumination, acquisition time = 0.05 s, *f*-stop = 16, focal plane = 5, FOV = 160 with no binning.

Following imaging, animals were dissected and selected tissues were collected to preweighed γ-counter tubes. Radioactivity of preweighed tissues and DUPA−^{99m}Tc (67 nmol, 150 μCi) in saline (100 μL) was counted in a γ-counter. CPM values were decay corrected, and results were calculated as % ID/gram of wet tissue and tumor-to-tissue ratios.

In Vitro Potency of DUPA−TubH. LNCaP cells were seeded into 24-well (50,000 cells/well in 500 μL) Falcon plates and allowed cells to form monolayers over 48 h. Spent medium was replaced with fresh medium (0.5 mL) containing increasing concentrations of DUPA−TubH in the presence or absence of 100-fold excess PMPA, and cells incubated for an additional 2 h at 37 °C. Cells were washed 3× with fresh medium and incubated in fresh medium (0.5 mL) for 66 h at 37 °C. Spent medium in each well was replaced with fresh medium (0.5 mL) containing [^{3}H]-thymidine (1 μCi/mL), and cells were incubated for 4 h at 37 °C to allow [^{3}H]-thymidine incorporation. Cells were then rinsed with medium (3× 0.5 mL) and treated with 5% trichloroacetic acid (0.5 mL) for 10 min at rt. Cells were dissolved in 0.25 M NaOH (0.5 mL), transferred into individual vials containing Ecolume scintillation cocktail (3.0 mL), and counted in a scintillation counter (Packard, Packard Instrument Company). IC_{50} was calculated by plotting % ^{3}H-thymidine incorporation versus log concentration of DUPA−TubH using GraphPad Prism 4.

In Vivo Potency of DUPA−TubH. Healthy male nu/nu mice were administered with multiple doses of freshly prepared DUPA−TubH dissolved in saline (200 μL) via lateral tail injection on days zero, 2, 4, 6, 8, and 10. Body weights and clinical observations were monitored prior to dosing and daily thereafter from day zero to 12. Chronic maximum tolerance dose was determined by plotting % weight change versus days on therapy, and any animals with a body weight loss of 20% or more over two consecutive days were euthanized.

Male nude mice bearing LNCaP xenograft tumors were then treated with 1.5 μmol/kg DUPA−TubH (for tumors of 90−130 mm^3) or 2.0 μmol/kg DUPA−TubH (for tumors of 320−360 mm^3) dissolved in 200 μL of saline via lateral tail vein injection. Treatments were conducted 3× per week for two weeks. Tumor volumes and body weights were measured on the same schedule. In vivo efficacy was evaluated by plotting tumor volume versus days on therapy.

Results

Design and Labeling of a PSMA-Targeted Radiotracer. In an effort to identify a high affinity targeting ligand for delivery of attached imaging and therapeutic agents to PSMA-expressing PCa cells, we conducted in silico docking studies on a series of PSMA inhibitors using a high resolution crystal structure of GCP-II in complex with the PSMA inhibitor termed GPI-18431 (PDB ID code 2C6C).[35] Due to its favorable binding mode (in silico), ease of synthesis, high experimental affinity for purified PSMA (K_i = 8 nM),[36] and availability of a free carboxylic acid not required for PSMA binding, 2-[3-(1,3-dicarboxypropyl)-ureido]pentanedioic acid (DUPA, Figure 1a) was selected as a possible targeting ligand.

Initial analysis of the tumor targeting specificity of DUPA-linked drugs required synthesis of a radiolabeled conjugate that would allow quantitation of its distribution in live animals. Because technetium (^{99m}Tc) is the major radioimaging nuclide used clinically, a common chelator of ^{99m}Tc, diaminopropionic acid-Asp-Cys,[32] was selected for attachment to DUPA. Thus, the PSMA crystal structure revealed a gradually narrowing access funnel 20 Å deep that extends from the protein surface to a binuclear zinc atom in the catalytic site.[35] By modeling the peptide spacer to fit the contours of this funnel, we were able to generate a targeting moiety that did not compromise DUPA's affinity for PSMA. Details and images of the fit of the peptide spacer to the 20

(35) Mesters, J. R.; Barinka, C.; Li, W. Structure of glutamate carboxypeptidase II, a drug target in neuronal damage and prostate cancer. *EMBO J.* **2006**, *25*, 1375–1384.

(36) Kozikowski, A. P.; Zhang, J.; Nan, F. Synthesis of urea-based inhibitors as active site probes of glutamate carboxypeptidase II: Efficacy as analgesic agents. *J. Med. Chem.* **2004**, *47*, 1729–1738.

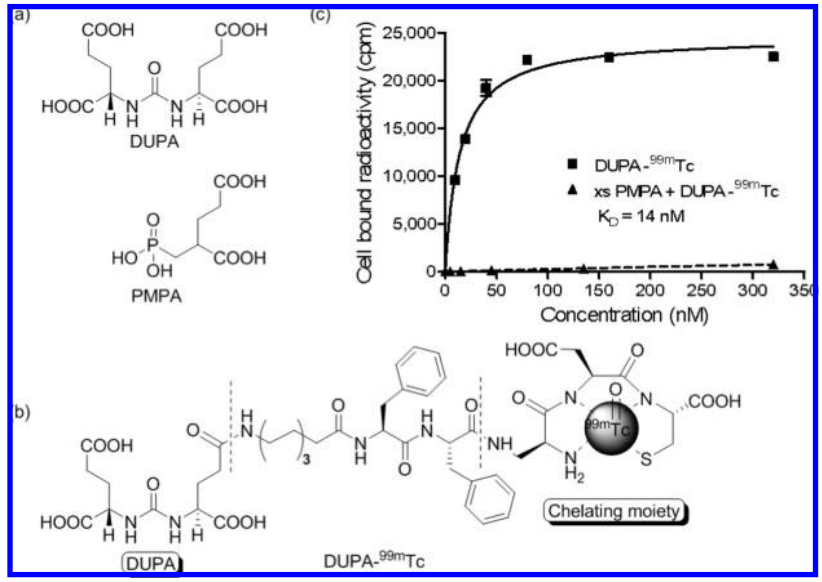

Figure 1. Structures of (a) PSMA inhibitors, DUPA and PMPA, (b) PSMA-targeted radiotracer, DUPA−^{99m}Tc. (c) Binding affinity and specificity of DUPA−^{99m}Tc to PSMA-positive LNCaP cells in culture. Error bars represent SD ($n = 3$).

Å deep tunnel leading to the DUPA binding site are presented in a companion paper, DOI 10.1021/mp9000712.[31]

Binding Affinity and Specificity of DUPA−^{99m}Tc. The affinity and specificity of the DUPA−^{99m}Tc radiotracer (Figure 1b) was first evaluated using LNCaP cells that express PSMA. The dissociation constant (K_D) derived from these studies was calculated to be 14 nM (Figure 1c). This binding affinity compares well with the K_I of DUPA for the purified enzyme (8 nM), suggesting that its conjugation to the chelating agent via the fitted peptide spacer does not extensively compromise its association with PSMA. The specificity of DUPA−^{99m}Tc for PSMA was next determined by coincubating LNCaP cells with the radioimaging agent in the presence of an excess (xs) of PMPA (blocked PSMA), a high affinity inhibitor of PSMA ($K_I = 0.3$ nM).[37] PMPA competed quantitatively with DUPA−^{99m}Tc for binding to LNCaP cells (Figure 1c), demonstrating that PSMA constitutes the sole DUPA−^{99m}Tc binding site on this cell line.

Binding and Internalization of Fluorescent Conjugates of DUPA. The ability of DUPA to deliver different cargos to PSMA on LNCaP cells was next evaluated by preparing DUPA conjugates of two fluorescent dyes and analyzing their binding and endocytosis by optical methods. LNCaP cells were incubated with DUPA−FITC (Figure 2a), DUPA−rhodamine B (Figure 2b), or DUPA−FITC in the presence of excess PMPA and analyzed by either flow cytometry or confocal fluorescence microscopy. DUPA−FITC was seen to efficiently label LNCaP cells in a manner that could be inhibited by excess PMPA (Figure 2c), suggesting that the fluorescent conjugate's binding was also PSMA-specific. More importantly, confocal microscopy revealed DUPA−FITC fluorescence only at the cell surface, whereas DUPA−rhodamine B fluorescence was seen throughout the LNCaP cell cytoplasm (Figure 2d). This apparent difference in intracellular distribution is informative, since FITC fluorescence is quenched at pHs < 6.2, while rhodamine B fluorescence is pH independent. Assuming both DUPA conjugates traffic through the same endosomes, these data suggest that DUPA conjugates are internalized and trafficked to acidic endosomes where FITC but not rhodamine B fluorescence is quenched.

Whole Body Imaging of Solid Tumor Xenografts. To further establish the specificity of our DUPA conjugates for PCa cells, DUPA−^{99m}Tc was injected into nude mice bearing LNCaP tumors on their shoulders. The targeted ^{99m}Tc radiotracer accumulated mainly in the PSMA-positive LNCaP tumor, with little or no radioactivity in other tissues except the kidneys (Figure 3a,c). Importantly, high levels of kidney uptake may be peculiar to the mouse, since immunocytochemical analyses and reported imaging studies of xenograft models suggest that PSMA expression is high in murine kidneys[19,23,26,28−30] but low in human kidneys.[16−18,22]

In vivo specificity of the PSMA-targeted imaging agent was further tested by prior administration of excess PMPA to block all PSMA sites (blocked PSMA) before DUPA−^{99m}Tc administration. Blocked LNCaP tumors display no DUPA−^{99m}Tc uptake (Figure 3b), confirming the specificity of the DUPA conjugate for PSMA in vivo. To further document this specificity, the radiotracer was also administered to two PSMA-negative mouse xenograft models [A549 (a human lung cancer cell line) and KB (a human nasopharyngeal cancer cell line)], and again whole body images were taken. As anticipated, no radioactivity was observed in either KB or A549 tumors (data not shown). Even after shielding the kidneys to detect low levels of DUPA−^{99m}Tc, no radioactivity was found in PSMA-negative and blocked PSMA tumors (Figure 3d−f). These studies thus confirm that very little DUPA−^{99m}Tc binding occurs to sites unrelated to PSMA in vivo.

(37) Jackson, P. F.; Slusher, B. S. Design of NAALADase: A novel neuroprotective strategy. *Curr. Med. Chem.* **2001**, *8*, 949–957.

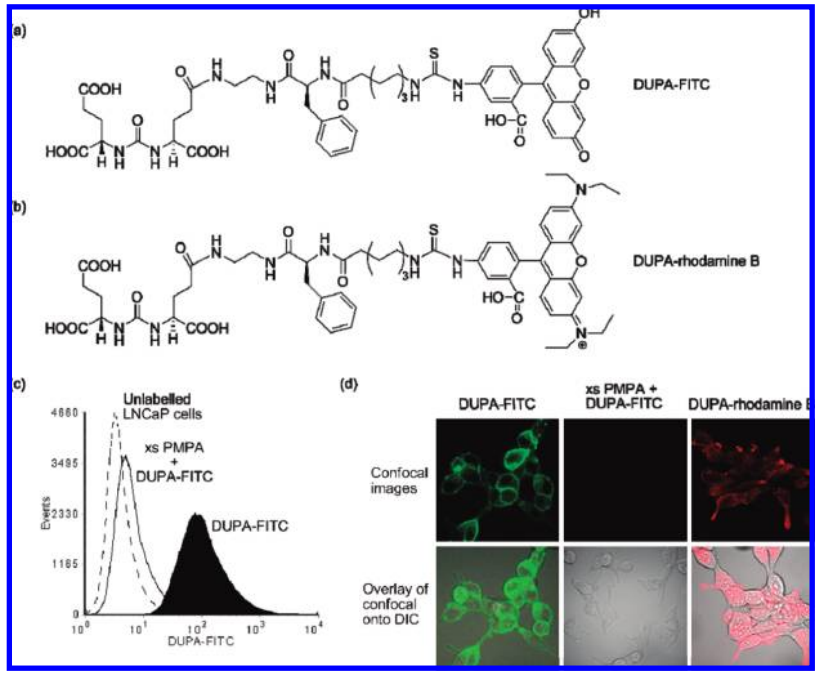

Figure 2. Structures of (a) DUPA−FITC and (b) DUPA−rhodamine B. Analysis of (c) binding of DUPA−FITC to LNCaP cells by flow cytometry and (d) binding and internalization of fluorescent DUPA conjugates to LNCaP cells by confocal microscopy in the presence and absence of excess PMPA. DIC = differential interference contrast images.

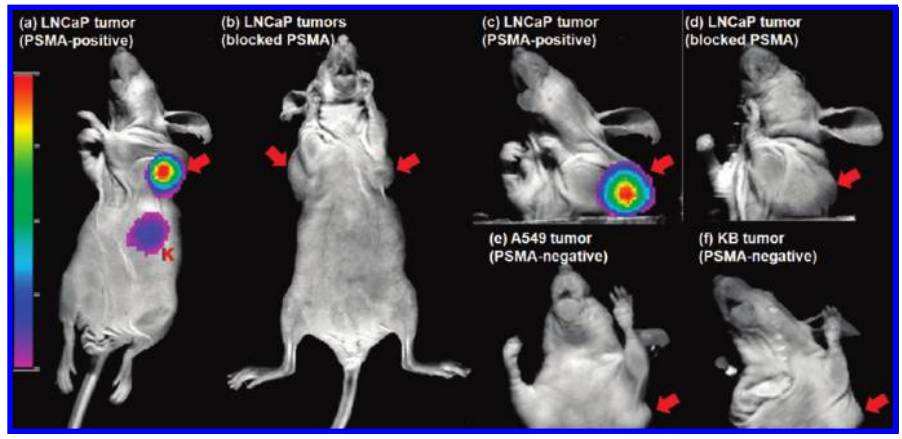

Figure 3. Overlay of whole-body radioimages on white light images of *nu/nu* mice bearing LNCaP, A549, or KB tumors 4 h after administration of DUPA−^{99m}Tc. In images (c−f), kidneys were shielded with lead pads. K = kidney, red arrows = solid tumor xenografts.

Analysis of DUPA−^{99m}Tc Biodistribution in Vivo. After imaging the animals, biodistribution studies were also conducted to quantitate DUPA conjugate specificity for PSMA in vivo. For this purpose, animals were sacrificed 4 h after administration of DUPA−^{99m}Tc and tissues were analyzed for radioactivity in a γ-counter. The highest percent injected dose per gram of wet tissue (% ID/g) was observed in the tumor (11.2%) and kidneys (28.9%) (Figure 4). Uptake in both tissues was strongly competable upon preinjection of PMPA, confirming the prominent expression of PSMA in both tissues. All other normal tissues displayed DUPA−^{99m}Tc uptake levels of <1% ID/g, resulting in excellent tumor-to-normal tissue ratios (see Figure 1 in the Supporting Information) of 75:1 (tumor:muscle), 73:1 (tumor:heart), 29:1 (tumor:skin), 18:1 (tumor:liver) and 17:1 (tumor:spleen). The fact that the tumor:blood ratio was 33:1 also suggests that the DUPA−^{99m}Tc conjugate has low serum protein binding and clears rapidly from the blood.

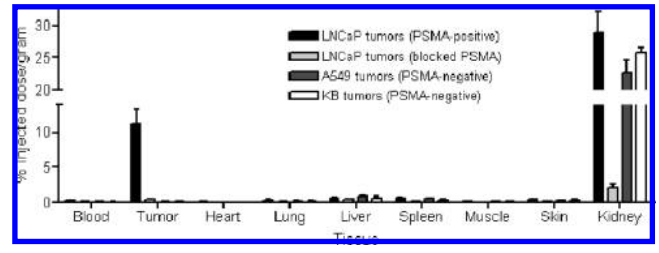

Figure 4. Biodistribution studies of DUPA−^{99m}Tc in *nu/nu* mice bearing LNCaP, A549, or KB tumors. Error bars represent SD (n = 5 mice/group).

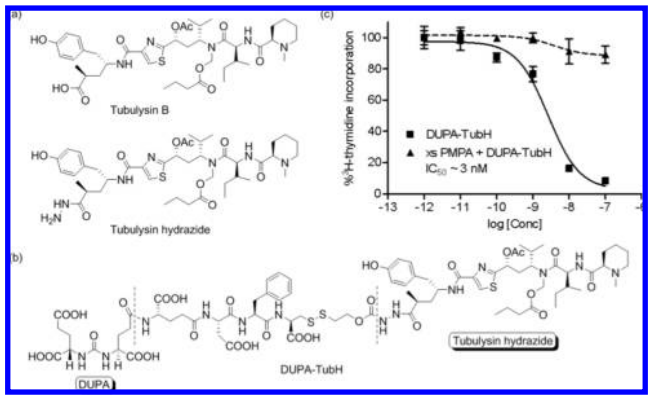

Figure 5. Structures of (a) tubulysin B and tubulysin hydrazide and (b) DUPA−TubH. (c) Evaluation of DUPA−TubH killing potency to LNCaP cells in culture. Error bars represent SD ($n = 3$).

In contrast to PSMA-expressing LNCaP tumors, PSMA-negative KB and A549 tumors exhibited minimal DUPA−^{99m}Tc uptake (Figure 4), despite their similar size and vascularity. These data confirm that retention of DUPA−^{99m}Tc in LNCaP tumors is not a consequence of a passive EPR (enhanced permeation and retention) effect, where tumors concentrate macromolecules from the blood due to their leaky vasculature and poorly developed lymphatic drainage.[38] The data also confirm that the neovasculature in murine tumors does not express PSMA, in contradistinction to the neovasculature in human tumors.[16,18]

Design and Analysis of a PSMA-Targeted Therapeutic Agent. The ability to deliver a variety of cargos to PSMA-expressing cells encouraged the development of a therapeutic conjugate of DUPA for use in treating PCa. To this end, DUPA was linked to tubulysin hydrazide (a derivative of tubulysin B, Figure 5a) microtubule inhibitor (tubulysin hydrazide, TubH) via a peptide spacer and disulfide bond. However, because TubH was so hydrophobic, one of the phenylalanines and part of the aliphatic spacer that were incorporated into the DUPA−^{99m}Tc linker to improve its fit within the PSMA tunnel had to be replaced with hydrophilic groups in order to maintain the solubility of the DUPA−TubH conjugate. Curiously, tubulysin B ($IC_{50} = 0.091-2.3$ nM),[39] a microtubule inhibitor, has exhibited too narrow a therapeutic window to be considered for clinical applications.[33] However, by converting its carboxylic acid group to a hydrazide, and targeting the modified tubulysin with a tumor-specific ligand, the therapeutic index of tubulysin B has been significantly improved without compromising its efficacy.[33] Based on these successful studies using folate as the targeting ligand,[33,40] it was hypothesized that an analogous DUPA conjugate of tubulysin B hydrazide would remain stable in circulation but release unmodified TubH following disulfide reduction within the endosomes[33] of the LNCaP cell.

To determine the in vitro efficacy of DUPA−TubH (Figure 5b), LNCaP cells were grown to 40% confluence and pulsed for 2 h with increasing concentrations of DUPA−TubH in the presence or absence of excess PMPA. After washing to remove unbound conjugate, cells were incubated an additional 66 h in fresh medium before analysis of tritiated thymidine incorporation. The aforementioned 2 h exposure was selected, since the DUPA conjugates were found to clear in vivo (from nontargeted tissues) in <2 h, suggesting that longer exposure to the conjugate might yield nonphysiological results. Thymidine incorporation (used as a measure of DNA synthesis) dramatically decreased with increasing concentrations of DUPA−TubH (Figure 5c). The IC_{50} value from the plot of % [^{3}H]-thymidine incorporation versus log concentration was calculated to be 3 nM. More importantly, DUPA−TubH cytotoxicity was nearly quantitatively blocked by excess PMPA, indicating that target cell killing was PSMA mediated. This finding was very encouraging, because it suggests that DUPA−TubH should not be toxic to PSMA-negative tissues.

Prior to conducting related cytotoxicity studies on live tumor-bearing mice, the maximum tolerated dose (MTD) of DUPA−TubH needed to be quantitated. A chronic MTD for DUPA−TubH was initially determined by repeated (3 injections/week for 2 weeks) tail vein injections of DUPA−TubH to be 3.0 μmol/kg. Efficacy of DUPA−TubH was then evaluated in mice bearing subcutaneous LNCaP tumor xenografts. LNCaP cells in HC Matrigel were implanted subcutaneously into male *nu/nu* mice and allowed to grow to either ~100 mm^3 or 330 mm^3 prior to initiation of treatment with 1.5 μmol/kg or 2.0 μmol/kg of DUPA−TubH, respectively. Untreated LNCaP tumors grew with a doubling time of <1 week and reached >1200 mm^3 by the end of the two week treatment period. In contrast, DUPA−TubH-treated mice showed tumor regression that was sustained (Figure 6a,c) until animals were euthanized for pathology. More importantly, antitumor activity was eliminated when binding of DUPA−TubH to PSMA was blocked by prior administration of excess PMPA, demonstrating the requirement for vacant PSMA receptors to achieve DUPA−TubH cytotoxicity. Importantly, body weights over the course of the study remained essentially unchanged (Figure 6b,d), suggesting that the therapy is not grossly toxic to the animals.

Discussion

The objectives of this study were to develop PSMA-targeted imaging and therapeutic agents for PCa cells. A radioimaging agent was constructed that demonstrates high

(38) Matsumura, Y.; Maeda, H. A new concept for macromolecular therapeutics in cancer chemotherapy: mechanism of tumoritropic accumulation of proteins and the antitumor agent smancs. *Cancer Res.* **1986**, *46*, 6387–6392.

(39) Steinmetz, H.; Glaser, N.; Herdtweck, E.; Sasse, F.; Reichenbach, H.; Hofle, G. Isolation, crystal and solution structure determination, and biosynthesis of tubulysins-powerful inhibitors of tubulin polymerization from myxobacteria. *Angew. Chem., Int. Ed.* **2004**, *43*, 4888–4892.

(40) Vlahov, I. R.; Wang, Y.; Kleindl, P. J.; Leamon, C. P. Design and regioselective synthesis of a new generation targeted chemotherapeutics. Part II: folic acid conjugates of tubulysins and their hydrazides. *Bioorg. Med. Chem. Lett.* **2008**, *18*, 4558–4561.

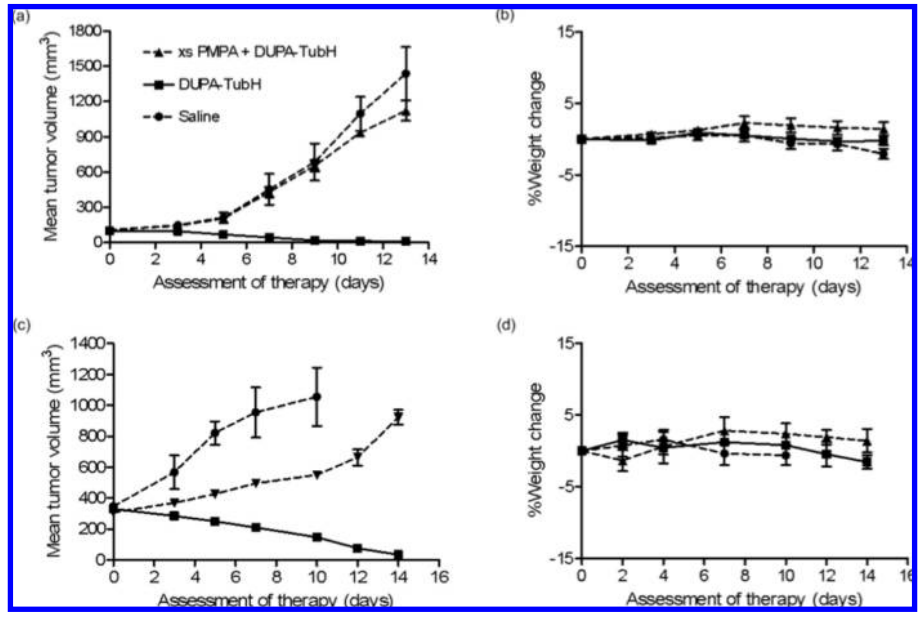

Figure 6. Effect of DUPA−TubH on the growth of subcutaneous LNCaP tumors, and on the weights of the treated mice. Mice treated with either 1.5 μmol/kg (a, b) or 2.0 μmol/kg (c, d) (■), untreated mice (●), treated mice preinjected with 100-fold (a, b) or 30-fold (c, d) excess of PMPA (▲). Error bars represent SD [$n = 4$ mice/group (a, c) or 3 mice/group (c, d)].

affinity and specificity for PSMA. Based on its ease of preparation and potential use in (i) locating metastatic disease, (ii) monitoring response to therapy, (iii) detecting disease recurrence following surgery, and (iv) selecting patients for subsequent DUPA−targeted chemotherapy, eventual use of DUPA−^{99m}Tc or a related PSMA-targeted radioimaging in the clinic seems promising.

Design and synthesis of a potent PSMA-targeted therapeutic agent was also achieved. Based on the high tumor-to-tissue uptake ratio of DUPA−^{99m}Tc, DUPA-targeted therapeutic agents were expected to show high tumor specificity. Indeed, DUPA−TubH was found to promote complete regression of established LNCaP tumors without causing weight loss in the treated animals. This apparent absence of toxicity was remarkable, since nontargeted tubulysin B is seen to have essentially no therapeutic window.[33] Thus, administration of 1.0 μmol/kg free TubH has been reported to kill tumor-bearing animals before it reduces their tumor volumes.[33] While detailed pathological analyses of DUPA−TubH treated mice will be required to establish any absence of toxicity, because PSMA expression in nonmalignant cells is primarily restricted to the kidneys, and since PSMA expression in kidneys is lower in humans than mice,[16−19] we hypothesize that any off-site toxicity seen in the mouse may be reduced in the human.

DUPA fluorescent conjugates were also demonstrated to bind LNCaP cells in a manner that was competable with excess PMPA. As we communicated elsewhere,[34] we also showed that these PSMA-targeted fluorophores bind and selectively label malignant cells in fresh peripheral blood samples from PCa patients. Because no fluorescent cells are detected in blood samples from healthy volunteers, a possible use of fluorescent DUPA conjugates could involve assessment of tumor burden or disease recurrence in PCa patients via quantitation of circulating tumor cells. And while fluorescence imaging has not yet achieved the prominence of radioimaging, future uses of DUPA−dye conjugates could conceivably also include detection and localization of malignant masses during surgery.

It has not escaped our attention that many other drugs and imaging agents could have been targeted to PCa cells with DUPA, including gene therapy vectors, antisense oligonucleotides, PET imaging agents, therapeutic siRNAs, liposomally entrapped drugs, immunotherapeutic agents and protein toxins. However, tubulysin, ^{99m}Tc, and the fluorescent dyes were selected for initial examination because of their potencies/sensitivities at low concentrations. Whether the capacity of the PSMA uptake pathway is sufficient to deliver effective quantities of less active therapeutic and imaging agents remains uncertain.

Finally, one might question the merit of developing a low molecular weight targeting ligand when monoclonal antibodies to PSMA are available. While monoclonal antibodies have distinct advantages,[15,16,18,22,41,42] they are also physically large ($M_r \sim 150{,}000$), penetrate solid tumors incompletely, and clear from nontargeted tissues slowly.[21,43] In contrast, DUPA is small ($M_r \sim 320$), can penetrate solid tumors rapidly, and clears from PSMA-negative tissues in

(41) Milowsky, M. I.; Nanus, D. M.; Kostakoglu, L. Vascular targeted therapy with anti-prostate-specific membrane antigen monoclonal antibody J591 in advanced solid tumors. *J. Clin. Oncol.* **2007**, *25*, 540–547.

(42) Bender, N. H.; Nanus, D. M.; Milowsky, M. I.; Kostakoglu, L.; Vallabajosula, S.; Goldsmith, S. J. Targeted systemic therapy of prostate cancer with monoclonal antibody to prostate-specific membrane antigen. *Semin. Oncol.* **2003**, *30*, 667–677.

<2 h. The monoclonal antibody, ^{111}In-Capromab pendetide (ProstaScint), is the only Food and Drug Administration (FDA) approved imaging agent for PCa. It binds to an intracellular epitope of PSMA in necrotic PCa cells. Unfortunately, it has shown high false positive results and has a low positive predicted value (PPV) for metastatic lymph node diseases and for the presence of PCa.[21,44] Additionally, ProstaScint has shown very poor tumor-to-muscle ratio (3:1) when compared to DUPA−^{99m}Tc (75:1) in the LNCaP xenograft model, indicating high nonspecific binding of the antibody.[44] While second generation antibodies (e.g., J591) which target the extracellular domain of PSMA may overcome some of these problems,[16,42] even these improved antibodies may retain some of the disadvantages of ProstaScint.[45,46]

Low molecular weight ligands of PSMA, on the other hand, are generally easy to synthesize and conjugate to therapeutic/imaging agents, easy to purify and characterize, compatible with both organic and aqueous solvents, and stable during storage. As noted in the Introduction, several radiolabeled inhibitors of PSMA have already been explored as imaging agents for PCa.[23] While the improved image qualities and shortened delay between imaging agent injection and image collection constitute significant advantages over ProstaScint, the long half-life of the ^{125}I-labeled inhibitor (~60 days) and the short half-life of the ^{11}C-labeled inhibitor (22 min) render eventual clinical use of these imaging agents problematic. During preparation of this manuscript for publication, however, three additional PSMA-targeted radioimaging agents with clinically useful characteristics were reported.[28−30] Both the ^{99m}Tc-labeled inhibitor and the two ^{18}F-labeled inhibitors display greater uptake in PSMA-negative organs than the DUPA−^{99m}Tc conjugate reported here. Further, these latter three targeted conjugates only transiently accumulate in the tumor, since by 2 h postinjection their tumor contents are reported to decline to 2.3, 3.7 and 0.2% ID/g, whereas the DUPA−^{99m}Tc conjugate remains at 11.2% ID/g at 4 h postinjection. This difference in tumor retention may account for the inability of a doxorubicin conjugate of the former inhibitor to kill PSMA-positive C4-2 cells even at higher concentration of 5 μM,[47] despite the fact that our DUPA−tubulysin conjugate killed LNCaP cells with an IC_{50} of 3 nM. Regardless, all of the aforementioned low molecular weight PSMA-targeted ligands show significant advantages over antibody-targeted imaging agents, raising the hope that the next PCa drug to enter the clinic might be targeted with a high affinity, low molecular weight PSMA-targeting ligand.

Acknowledgment. We thank Wilfredo Ayala-Lopez for assisting with the Kodak Imaging Station studies, and Wei He for assisting with confocal studies. This work was supported by a grant from Endocyte, Inc.

Supporting Information Available: Plots of tumor-to-normal tissue ratios of DUPA−^{99m}Tc in *nu/nu* mice bearing LNCaP tumors. This material is available free of charge via the Internet at http://pubs.acs.org.

MP900069D

(43) Ponsky, L. E.; Cherullo, E. E.; Starkey, R.; Nelson, D.; Neumann, D.; Zipper, C. P. Evaluation of preoperative ProstaScint scans in the prediction of nodal disease. *Prostate Cancer Prostatic Dis.* **2002**, *5*, 132–135.

(44) Tasch, J.; Gong, M.; Sadelain, M.; Heston, W. D. A unique folate hydrolase, prostate-specific membrane antigen (PSMA): a target for immunotherapy. *Crit. Rev. Immunol.* **2001**, *21*, 249–261.

(45) Seccamani, E.; Tattanelli, M.; Mariani, M.; Spranzi, E.; Scassellati, G. A.; Siccardi, A. G. A simple qualitative determination of human antibodies to murine immunoglobulins (HAMA) in serum samples. *Nucl. Med. Biol.* **1989**, *16*, 167–170.

(46) Colcher, D.; Bird, R.; Rosell, M. In vivo tumor targeting of a recombinant single-chain antigen-binding protein. *J. Natl. Cancer Inst.* **1990**, *82*, 1191–1197.

(47) Jayaprakash, S.; Wang, X.; Heston, W. D.; Kozikowski, A. P. Design and synthesis of a PSMA inhibitor-doxorubicin conjugate for targeted prostate cancer therapy. *ChemMedChem* **2006**, *1*, 299–302.